

**H<sub>2</sub>-assisted ternary recombination of H<sub>3</sub><sup>+</sup> with electrons at 300 K**Petr Dohnal,<sup>1</sup> Peter Rubovič,<sup>1</sup> Ábel Kálosi,<sup>1</sup> Michal Hejduk,<sup>1</sup> Radek Plašil,<sup>1</sup> Rainer Johnsen,<sup>2</sup> and Juraj Glosík<sup>1</sup><sup>1</sup>*Department of Surface and Plasma Science, Faculty of Mathematics and Physics, Charles University in Prague, Prague 18000, Czech Republic*<sup>2</sup>*Department of Physics and Astronomy, University of Pittsburgh, Pittsburgh, Pennsylvania 15260, USA*

(Received 12 March 2014; revised manuscript received 27 August 2014; published 16 October 2014)

Stationary afterglow measurements in conjunction with near-infrared absorption spectroscopy show that the recombination of the H<sub>3</sub><sup>+</sup> ion with electrons in ionized gas mixtures of He, Ar, and H<sub>2</sub> at 300 K is strongly enhanced by neutral helium and by molecular hydrogen. The H<sub>2</sub>-assisted ternary recombination coefficient  $K_{\text{H}_2} = (8.7 \pm 1.5) \times 10^{-23} \text{ cm}^6 \text{ s}^{-1}$  substantially exceeds the value measured for H<sub>3</sub><sup>+</sup> in ambient helium ( $K_{\text{He}} \sim 10^{-25} \text{ cm}^6 \text{ s}^{-1}$ ) or predicted by the generally accepted classical theory of Bates and Khare ( $\sim 10^{-27} \text{ cm}^6 \text{ s}^{-1}$ ) for atomic ions. Because of the extremely large value of  $K_{\text{H}_2}$  in a hydrogen plasma the ternary recombination dominates over binary recombination already at pressures above 3 Pa. This can have consequences in plasma physics, astrophysics, recombination pumped lasers, plasma spectroscopy, plasmatic technologies, etc. The ternary processes provide a plausible explanation for the discrepancies between many earlier experimental results on H<sub>3</sub><sup>+</sup> recombination. The observation that the ternary process saturates at high He and H<sub>2</sub> densities suggests that recombination proceeds by a two-step process: formation of a long-lived complex [with a rate coefficient  $\alpha_F = (1.5 \pm 0.1) \times 10^{-7} \text{ cm}^3 \text{ s}^{-1}$ ] followed by collisional stabilization.

DOI: [10.1103/PhysRevA.90.042708](https://doi.org/10.1103/PhysRevA.90.042708)

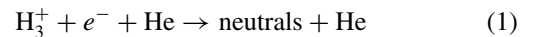
PACS number(s): 34.80.Lx, 42.62.Fi, 52.20.Hv

**I. INTRODUCTION**

The triatomic hydrogen ion occupies a special position in molecular physics, in physical chemistry, and in astrophysics. This simple ion, whose very existence was once doubted, is now recognized as the most abundantly produced molecular ion in the universe. It not only plays a pivotal role in the molecular evolution of some interstellar clouds but also provides a tool for measuring their temperatures [1]. The recombination of the H<sub>3</sub><sup>+</sup> ion with electrons is of interest for modeling hydrogen-containing plasmas and, in part for this reason, has been studied experimentally and theoretically for over 60 years [2]. Many extensive laboratory studies have been performed to clarify the formation and destruction processes of H<sub>3</sub><sup>+</sup>, in particular the recombination of H<sub>3</sub><sup>+</sup> with electrons at low temperatures [2,3]. The word “enigma” appeared frequently in publications [4] because the measured recombination rate coefficients differed by several orders of magnitude (see extended discussion in [2,3]). The principal current motivation for H<sub>3</sub><sup>+</sup> recombination studies comes from the physics and chemistry of diffuse astrophysical clouds and planetary ionospheres (see discussion in [5–7]). H<sub>3</sub><sup>+</sup> was observed spectroscopically in the laboratory in 1980 [8], but it took many years until it was detected in emission spectra from Jupiter [9], Saturn, and Uranus (see discussion in [10]), and in interstellar plasmas [11,12].

In 2001 a new theory of H<sub>3</sub><sup>+</sup> recombination was developed [13,14] and it became clear afterwards that para-H<sub>3</sub><sup>+</sup> and ortho-H<sub>3</sub><sup>+</sup> behave differently [15]. Storage rings were used in corresponding state selected studies [2]. For temperatures above 300 K the agreement between theory and the most recent storage ring experiments [16–19] is excellent but data at lower temperatures are still not quite conclusive because internal states of the recombining ions are not necessarily in thermal equilibrium [20]. It is now generally accepted that recombination of H<sub>3</sub><sup>+</sup> occurs with a binary rate coefficient of  $\alpha_{\text{bin}}(300 \text{ K}) \sim 6 \times 10^{-8} \text{ cm}^3 \text{ s}^{-1}$  [21]. For applications to low-density astrophysical clouds it is the binary coefficient that matters.

The fact remains that many well-executed plasma afterglow experiments gave recombination rates that were larger by factors of 3 to 4 than the theoretical and storage ring data. A better understanding was achieved after the discovery of fast helium-assisted ternary recombination of H<sub>3</sub><sup>+</sup> in afterglow plasma in a He-Ar-H<sub>2</sub> gas mixture [22,23]. It was then found that the ternary He-assisted recombination process



is indeed very effective, exceeding by over two orders of magnitude (at 300 K) the value predicted by the classical treatment of Bates and Khare [24]. The much faster ternary recombination of H<sub>3</sub><sup>+</sup> has been attributed to formation of long-lived rotationally excited neutral H<sub>3</sub><sup>#</sup> Rydberg molecules and subsequent collisions with helium atoms [22,23] that eventually lead to dissociation into neutral products. We note that the formation of H<sub>3</sub><sup>#</sup> Rydberg states has also been invoked as a mechanism in a recombination-pumped laser in H<sub>3</sub><sup>+</sup> containing plasma [25].

The recombination of the H<sub>3</sub><sup>+</sup> ion has been studied in our laboratory for almost 15 years. During those years, several different stationary afterglow (Advanced Integrated Stationary Afterglow (AISA) [26], Stationary Afterglow with Cavity Ring Down Spectrometer (SA-CRDS) [27,28]) and flowing afterglow (Flowing Afterglow with Langmuir Probe (FALP) [29], Cryo-FALP [21,23,30]) experiments were employed to study the H<sub>3</sub><sup>+</sup> recombination process in low-temperature afterglow plasma in a He-Ar-H<sub>2</sub> gas mixture. The main differences are in the range of covered number densities of He and H<sub>2</sub>, in the electron and ion densities, in the covered temperature range, in the time scale of monitored plasma decay, and in applied diagnostics (see, e.g., [23]). A broad range of the measured plasma parameters is necessary to study the dependence of the measured effective recombination rate coefficient  $\alpha_{\text{eff}}$  on plasma parameters and eventually to determine rate coefficients for binary and ternary recombination of H<sub>3</sub><sup>+</sup> ions and their temperature dependences. This procedure is necessary

especially in the case of the  $\text{H}_3^+$  ion, where long-lived highly excited neutral  $\text{H}_3$  can be formed in collision of  $\text{H}_3^+$  with electrons [22,23]. Very extensive and systematic studies are required because the afterglow plasmas are influenced also by formation and relaxation processes and also by ambipolar diffusion and these processes depend on the same parameters as the effective recombination rate coefficient.

We should mention here that in early AISA experiments (stationary afterglow with Langmuir probe and mass spectrometer [26]) we observed a rapid fall off of value of measured effective recombination rate coefficient  $\alpha_{\text{eff}}$  at  $[\text{H}_2] \ll 10^{12} \text{ cm}^{-3}$ , where newly formed  $\text{H}_3^+$  ions undergo on average less than one collision with  $\text{H}_2$  prior to its recombination. The mass spectra obtained during the experiment showed that  $\text{H}_3^+$  was the dominant ion species but the internal state of the ions was not probed in the AISA experiments. We do not have a certain explanation for this observation (see discussion in [23,31]). In later experiments we used  $10^{12} < [\text{H}_2] < 5 \times 10^{13} \text{ cm}^{-3}$ ; the measured  $\alpha_{\text{eff}}$  did not change with  $[\text{H}_2]$  (in the context of those experiments we called it the “saturated region”, see [23,31]). At these conditions the formed  $\text{H}_3^+$  ions have many collisions with  $\text{H}_2$  and He prior to their recombination. We found that the measured  $\alpha_{\text{eff}}$  depends linearly on helium number density;  $\alpha_{\text{eff}} = \alpha_{\text{bin}} + K_{\text{He}}[\text{He}]$  in the “saturated region.” The binary rate coefficient was determined from the low-pressure limit as  $\alpha_{\text{bin}} = \alpha_{\text{eff}}([\text{He}] \rightarrow 0)$ . The obtained binary recombination rate coefficients are very close to the theoretically predicted value [15] and the value reported by storage ion ring CRYRING [18]. Using SA-CRDS we confirmed that  $\text{H}_3^+$  ions in recombination dominated afterglow plasmas are in thermal equilibrium with He [32]. All these later studies were performed for  $[\text{H}_2]$  higher than  $10^{12} \text{ cm}^{-3}$  but low enough to prevent formation of fast recombining  $\text{H}_5^+$  ions.

There are good reasons to believe that hydrogen molecules should be more efficient than inert helium atoms in promoting  $\text{H}_3^+$  recombination, and there is some earlier experimental evidence in support of this expectation [29,30,33,34]. However, the effect of  $\text{H}_2$  has not been studied systematically and this is the first study dedicated to  $\text{H}_2$ -assisted ternary recombination.

## II. EXPERIMENT

The technical details of the stationary-afterglow cavity-ring-down-spectroscopy apparatus (SA-CRDS) have been adequately described elsewhere [27]. The plasma is formed in a pulsed microwave discharge in a mixture of He, Ar, and  $\text{H}_2$  and the densities of three rotational states of the ground vibrational state of  $\text{H}_3^+$  during the afterglow are measured using the transitions  $3\nu_2^1(2,0) \leftarrow 0\nu_2^0(1,0)$  and  $3\nu_2^1(4,3) \leftarrow 0\nu_2^0(3,3)$  for ortho- $\text{H}_3^+$  and  $3\nu_2^1(2,1) \leftarrow 0\nu_2^0(1,1)$  for para- $\text{H}_3^+$ . Details and notation are discussed in [32,35,36]. The kinetic temperature of the ions is obtained by measuring Doppler broadening of the absorption lines and the rotational temperature is obtained from the relative populations of measured states (for details see [32]). A numerical model of the chemical kinetics is used to determine the most appropriate conditions for the experiment. A water transition at  $7236.45 \text{ cm}^{-1}$  (line position taken from HITRAN database [37]) was routinely scanned to estimate the amount of  $\text{H}_2\text{O}$  impurities in the apparatus. Typically, the

water vapor concentration was at a safe level of less than  $5 \times 10^{10} \text{ cm}^{-3}$  (less than 0.1 ppm of buffer gas number density).

The present experimental study focus on  $\text{H}_2$ -assisted recombination of  $\text{H}_3^+$  ions. Ternary recombination rate coefficients were derived from the measured ion number density decays with an effective recombination rate coefficient  $\alpha_{\text{eff-ion}}$  for a wide range of  $[\text{He}]$  and  $[\text{H}_2]$  densities. For details on the data analysis see [32].

## III. COMPLEX MODEL OF TERNARY RECOMBINATION

Ternary contributions in  $\text{H}_3^+$  recombination can occur by formation of Rydberg molecules  $\text{H}_3^\#$  by resonant capture of an electron into a rotationally excited Rydberg state with the formation rate coefficient  $\alpha_F$ . The unstable molecule (or “complex”) can decay during its lifetime by autoionization with a time constant  $\tau_a$  or it can be “stabilized” (rendered incapable of being autoionized or being collisionally reionized) with rate coefficient  $k_{\text{SM}}$  in a collision with a third particle M of number density  $[\text{M}]$ . Provided that the lifetime  $\tau_a$  is much shorter than the time scale of the plasma decay, the number density ratio  $[\text{H}_3^\#]/[\text{H}_3^+]$  can be taken as constant and the effective recombination coefficient for  $\text{H}_3^+$  dominated plasma becomes

$$\alpha_{\text{eff-ion}} = \alpha_{\text{bin}} + \alpha_F \frac{k_{\text{SM}}[\text{M}]}{1/\tau_a + k_{\text{SM}}[\text{M}]} \quad (2)$$

This model of ternary recombination is similar to that proposed in our earlier publications [22,23,30]. We introduce the three-body recombination rate coefficient  $K_M$  defined as  $K_M = \alpha_F k_{\text{SM}} \tau_a$ . In the limit of small  $[\text{M}]$  (the “linear” regime) the second term of Eq. (2) reduces to  $K_M[\text{M}]$ . In the limit of large  $[\text{M}]$ , the second term of Eq. (2) approaches the constant value  $\alpha_F$  and the three-body recombination process is then said to “saturate.” This brief discussion hides a great amount of detail. In reality, one should consider an ensemble of many complexes, and more than two steps may be required to stabilize the complexes. In the experiment both He and  $\text{H}_2$  can act as neutral third bodies. If one assumes that both gases act on the same complexes, the product  $K_M[\text{M}]$  can be replaced by the sum  $K_{\text{H}_2}[\text{H}_2] + K_{\text{He}}[\text{He}]$ . We assume these contributions to be additive. We also assume that binary and ternary recombination are purely additive. This is not necessarily true if both processes share the same initial states.

The proposed simplified recombination mechanism is summarized in Fig. 1, where  $k_{\text{SHe}}$  and  $k_{\text{SH}_2}$  are the binary rate coefficients for collisional stabilization of  $\text{H}_3^\#$  in collisions with He and  $\text{H}_2$ , respectively. The ternary recombination rate coefficients for He- and  $\text{H}_2$ -assisted recombination

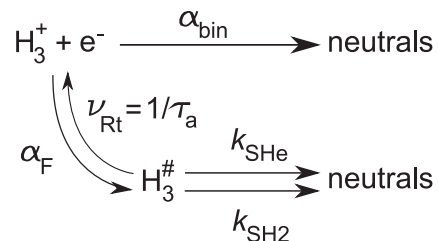


FIG. 1. The scheme of the proposed  $\text{H}_3^+$  recombination mechanism. Used symbols are explained in the text.

( $K_{\text{He}}$  and  $K_{\text{H}_2}$ , respectively) are introduced as  $K_{\text{He}} = \alpha_{\text{F}} k_{\text{SHe}} \tau_{\text{a}}$  and  $K_{\text{H}_2} = \alpha_{\text{F}} k_{\text{SH}_2} \tau_{\text{a}}$ .

There is one additional recombination process that can make a contribution at high  $[\text{H}_2]$ : The  $\text{H}_3^+$  ions are known to enter a chemical equilibrium with weakly bound  $\text{H}_5^+$  cluster ions that recombine very fast at 300 K ( $\alpha_5 \sim 2 \times 10^{-6} \text{ cm}^3 \text{ s}^{-1}$ ) [38,39]. At 300 K, the clustering equilibrium constant, defined by  $[\text{H}_5^+]/[\text{H}_3^+] = K_{\text{C}}[\text{H}_2]$ , has a value  $K_{\text{C}}(300 \text{ K}) = 6.7 \times 10^{-19} \text{ cm}^3$  [40]. Even at the highest  $\text{H}_2$  concentrations ( $6 \times 10^{16} \text{ cm}^{-3}$ ) used in present experiments less than 4% of the  $\text{H}_3^+$  ions are clustered.

To a good approximation, the effective recombination rate coefficient can then be written as

$$\alpha_{\text{eff-ion}} = \alpha_{\text{bin}} + \alpha_{\text{F}} \frac{K_{\text{He}}[\text{He}] + K_{\text{H}_2}[\text{H}_2]}{\alpha_{\text{F}} + K_{\text{He}}[\text{He}] + K_{\text{H}_2}[\text{H}_2]} + \alpha_5 K_{\text{C}}[\text{H}_2]. \quad (3)$$

A more rigorous kinetic analysis, that includes recombination of  $\text{H}_5^+$ , shows that the relative abundance of  $\text{H}_5^+$  in recombining plasmas is smaller by about a factor of 2 than  $K_{\text{C}}[\text{H}_2]$  and that it varies with electron density.

Equation (3) implies that  $\alpha_{\text{eff-ion}}$  saturates at the value  $\alpha_{\text{bin}} + \alpha_{\text{F}}$  if  $\alpha_{\text{F}} \ll (K_{\text{He}}[\text{He}] + K_{\text{H}_2}[\text{H}_2])$ . While in previous  $\text{H}_3^+$  experiments [21–23,31,32] the range of  $[\text{He}]$  was too small to detect saturation, the present experiments clearly exhibit saturation (details to be given below). Also, a slight dependence on  $[\text{H}_2]$  was observed in the earlier experiments [29,33,38] but it was then thought to arise from formation of fast recombining  $\text{H}_5^+$  ions at higher  $[\text{H}_2] > 10^{14} \text{ cm}^{-3}$ . However,  $\text{H}_5^+$  formation at temperatures near 300 K does not suffice to explain the increase of the recombination rate coefficient dependent on  $[\text{H}_2]$  at 300 K (with  $[\text{H}_2] < 2 \times 10^{15} \text{ cm}^{-3}$ ) that was also observed by Gougousi *et al.* [33]. On the other hand, Amano's [34] spectroscopic studies in a stationary afterglow experiment in pure hydrogen yielded an  $\text{H}_3^+$  recombination rate coefficient that was independent of  $\text{H}_2$  density, but three times larger than the currently accepted binary recombination rate coefficient [2].

#### IV. EXPERIMENTAL DATA AND RESULTS

Figure 2 shows typical  $\text{H}_3^+$  decay curves measured by SA-CRDS and the calculated densities of  $\text{H}_3^+$  and  $\text{H}_5^+$  ions. The rate coefficients  $\alpha_{\text{eff-ion}}$  are obtained by fitting the decay of the  $\text{H}_3^+$  number densities, taken as the sum of those in the ortho and para states assuming thermal equilibrium (see discussion in [32]), or calculated from the population of the ortho- $\text{H}_3^+$  (1,0) state only. No substantial difference between these two evaluations was observed.

The chemical kinetics calculations solve the set of reactions as described by Plašil *et al.* [26]. Because the composition of the plasma at the end of the microwave pulse is difficult to ascertain, the calculations were performed for many sets of different initial conditions. The results of the model show that at the number densities of He, Ar, and  $\text{H}_2$  used in present experiments the  $\text{H}_3^+$  ion becomes the dominant ion species within 150  $\mu\text{s}$  after switching off the discharge. An example is displayed in Fig. 2 for the following initial conditions in quasineutral plasma:  $[\text{H}_3^+] = n_{\text{e}}$ ;  $[\text{He}^{\text{m}}] = 1 \times 10^{11} \text{ cm}^{-3}$ , where  $[\text{He}^{\text{m}}]$  is the number density of metastable helium

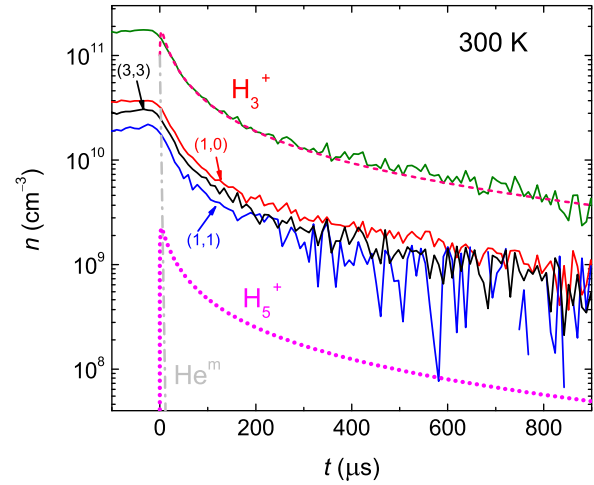


FIG. 2. (Color online) The decay curves measured for (1,0), (1,1), and (3,3) states of  $\text{H}_3^+$  at 300 K and number densities  $[\text{He}] = 8 \times 10^{17} \text{ cm}^{-3}$ ,  $[\text{H}_2] = 2 \times 10^{16} \text{ cm}^{-3}$ , and  $[\text{Ar}] = 7 \times 10^{14} \text{ cm}^{-3}$ . The total number density of  $\text{H}_3^+$  ions, calculated from the measured data under assumption of LTE, is shown as a full line. Calculated evolutions of the number densities of  $\text{H}_3^+$ ,  $\text{H}_5^+$ , and  $\text{He}^{\text{m}}$  are indicated as dashed, dotted, and dash-dotted lines, respectively.

atoms. For illustration of the result of the model, the measured evolutions of the number density of (1,0), (1,1), and (3,3) states of the  $\text{H}_3^+$  ion and of the overall number density of the  $\text{H}_3^+$  ion are also plotted in Fig. 2. The most important reactions taking place in the formation of  $\text{H}_3^+$  are listed in Table II of [26]. A fast decay of helium metastables  $\text{He}^{\text{m}}$  is given by Penning ionization with  $\text{H}_2$  and Ar. The  $\text{H}_3^+$  recombination rate coefficient was taken from the present data and the  $\text{H}_5^+$  recombination rate coefficient at 300 K was taken as  $\alpha_5 \sim 2 \times 10^{-6} \text{ cm}^3 \text{ s}^{-1}$  [38,39].

A large set of decay curves at 300 K, similar to those in Fig. 2, were recorded and analyzed for a wide range of  $[\text{H}_2]$  and for several  $[\text{He}]$ . The dependences of  $\alpha_{\text{eff-ion}}$  on  $[\text{H}_2]$  at particular  $[\text{He}]$  are shown in Fig. 3. The value obtained in pure  $\text{H}_2$  using the same experimental setup at  $(270 \pm 5) \text{ K}$  is also included (full diamond).

The binary rate coefficient,  $\alpha_{\text{bin}}(300 \text{ K}) = 6 \times 10^{-8} \text{ cm}^3 \text{ s}^{-1}$ , is known from previous SA-CRDS and Cryo-FALP experiments [21]. To emphasize the ternary contribution we subtracted the value of  $\alpha_{\text{bin}}$  from the measured  $\alpha_{\text{eff-ion}}$  and only the difference  $\alpha_{\text{eff-ion}} - \alpha_{\text{bin}}$  corresponding to the ternary contribution is shown in Fig. 3. The data clearly show that  $\alpha_{\text{eff-ion}} - \alpha_{\text{bin}}$  rises with increasing  $[\text{H}_2]$  up to  $[\text{H}_2] \sim 10^{16} \text{ cm}^{-3}$  and then saturates, as expected from the complex formation model [see Eq. (3)]. Two estimates of the contribution due to formation and subsequent recombination of  $\text{H}_5^+$  ions to the overall measured recombination rate coefficient are displayed in Fig. 3. The line denoted  $\text{LTE}_{\text{H}_5}$  shows the product of  $\alpha_5 K_{\text{C}}[\text{H}_2]$ , i.e.,  $\text{H}_5^+$  is assumed to be in thermal equilibrium with  $\text{H}_3^+$  and the  $[\text{H}_5^+]/[\text{H}_3^+]$  ratio is approximated using an equilibrium constant of  $K_{\text{C}}(300 \text{ K}) = 6.7 \times 10^{-19} \text{ cm}^3$  [40]. A considerably smaller and more realistic contribution of  $\text{H}_5^+$  (the line marked  $\text{M}_{\text{H}_5}$ ) is obtained from our kinetic model that includes the recombination loss of  $\text{H}_5^+$ . The comparison

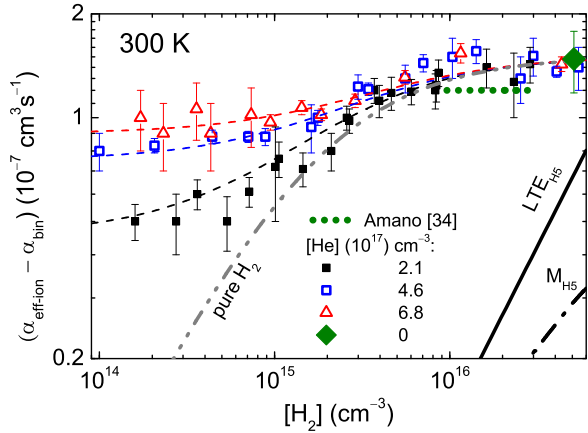


FIG. 3. (Color online) The dependencies of  $(\alpha_{\text{eff-ion}} - \alpha_{\text{bin}})$  on  $[\text{H}_2]$  measured at indicated  $[\text{He}]$ . Full diamond: measurements in pure  $\text{H}_2$ . Dashed lines: fits of Eq. (3) to the data, using the parameters mentioned in the text. Double-dot-dashed line: three-body recombination in pure  $\text{H}_2$ . Solid line ( $\text{LTE}_{\text{H}_5^+}$ ): approximate  $\text{H}_5^+$  contribution,  $\alpha_5 K_C [\text{H}_2]$ . Dash-dotted line ( $M_{\text{H}_5}$ ):  $\text{H}_5^+$  contribution obtained from the kinetic model for  $[\text{He}] = 2.1 \times 10^{17} \text{ cm}^{-3}$ . Dotted horizontal line: data obtained by Amano [34] in pure  $\text{H}_2$  at 273 K, after subtracting  $\alpha_{\text{bin}} = 6 \times 10^{-8} \text{ cm}^3 \text{ s}^{-1}$ .

of the measured  $\alpha_{\text{eff-ion}}$  with calculated contributions ( $\text{LTE}_{\text{H}_5^+}$  and  $M_{\text{H}_5}$ ) indicates that the actual contribution due to  $\text{H}_5^+$  formation is negligible at  $[\text{H}_2] < 2 \times 10^{16} \text{ cm}^{-3}$ . We fitted the measured  $\alpha_{\text{eff-ion}}$  by Eq. (3), neglecting contribution from  $\text{H}_5^+$  formation and using  $\alpha_{\text{bin}} = 6 \times 10^{-8} \text{ cm}^3 \text{ s}^{-1}$ ; see the dashed lines in the Fig. 3. The inferred rate coefficients are  $K_{\text{He}} = (3.3 \pm 0.7) \times 10^{-25} \text{ cm}^6 \text{ s}^{-1}$ ,  $K_{\text{H}_2} = (8.7 \pm 1.5) \times 10^{-23} \text{ cm}^6 \text{ s}^{-1}$ , and  $\alpha_F = (1.5 \pm 0.1) \times 10^{-7} \text{ cm}^3 \text{ s}^{-1}$ . Substituting these rate constants into Eq. (3) we derived  $(\alpha_{\text{eff-ion}} - \alpha_{\text{bin}})$  for the ternary recombination in pure  $\text{H}_2$ . This gives the double-dot-dashed line labeled “pure  $\text{H}_2$ ” in Fig. 3.

For comparison we also include in Fig. 3 the values obtained by Amano [34] in his spectroscopic study of  $\text{H}_3^+$  recombination in afterglow plasma in pure  $\text{H}_2$  at 273 K. The binary contribution has been subtracted. Amano’s results agree quite well with our data, strongly suggesting that Amano measured in the saturated region.

For consistency and for comparison with previous experiments we remeasured the dependence of  $\alpha_{\text{eff-ion}}$  on  $[\text{He}]$  up to  $[\text{He}] = 8 \times 10^{17} \text{ cm}^{-3}$  at a low hydrogen density,  $[\text{H}_2] = 2 \times 10^{14} \text{ cm}^{-3}$ , and at 100 times higher density,  $[\text{H}_2] = 2 \times 10^{16} \text{ cm}^{-3}$ . The obtained values can be seen in Fig. 4. At low  $[\text{H}_2]$ ,  $\alpha_{\text{eff-ion}}$  increases with increasing  $[\text{He}]$  and approaches saturation at very high  $[\text{He}]$ . At high  $[\text{H}_2]$   $\alpha_{\text{eff-ion}}$  is nearly constant at the value  $\alpha_F$  obtained by fitting the data in Fig. 3. The agreement of the present SA-CRDS values with those obtained in the Cryo-FALP experiment [23] is noteworthy since the electron densities in those experiments differed by more than a factor of 10. The errors in Figs. 3 and 4 are statistical errors of the fits to the time decay of  $[\text{H}_3^+]$ . The systematic error is estimated as 10%.

To show the difference between the helium- and hydrogen-assisted ternary recombination of the  $\text{H}_3^+$  ion, the dependences of  $\alpha_{\text{eff-ion}}$  on  $[\text{He}]$  and  $[\text{H}_2]$  are plotted in Fig. 5 together

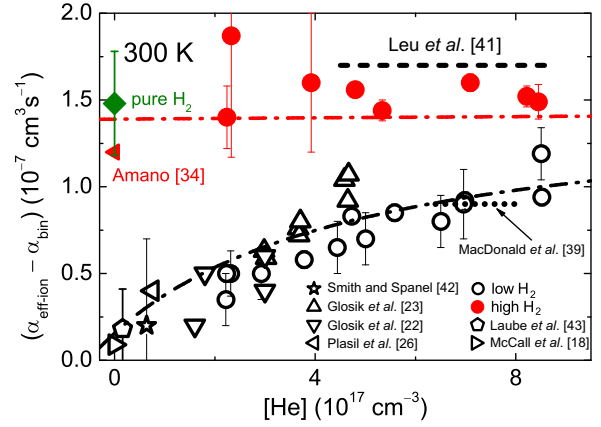


FIG. 4. (Color online) Measured dependence of  $(\alpha_{\text{eff-ion}} - \alpha_{\text{bin}})$  on He number density at 300 K for  $[\text{H}_2] = 2 \times 10^{14} \text{ cm}^{-3}$  (open circles) and for  $[\text{H}_2] = 2 \times 10^{16} \text{ cm}^{-3}$  (closed circles). The values of  $(\alpha_{\text{eff-ion}} - \alpha_{\text{bin}})$  measured in pure  $\text{H}_2$  at  $(270 \pm 5) \text{ K}$  are denoted by full diamonds (see also Fig. 3). The values measured in other experiments [18,22,23,26,34,39,41–43] are plotted for comparison. Values indicated by open symbols were measured for  $[\text{H}_2] < 5 \times 10^{14} \text{ cm}^{-3}$ . All experiments were performed with helium as a buffer gas with the exception of data in [18,34,39] where no buffer gas, pure  $\text{H}_2$ , or neon buffer gas was used, respectively. The dot-dashed lines denote values given by Eq. (3) for  $[\text{H}_2] = 2 \times 10^{14}$  and  $2 \times 10^{16} \text{ cm}^{-3}$  and with parameters written in the text.

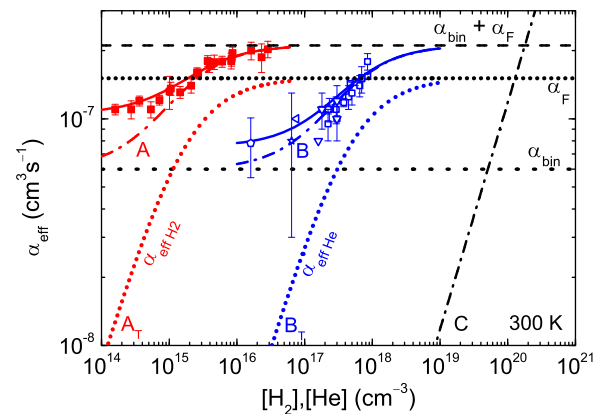


FIG. 5. (Color online) Measured dependence of the effective recombination rate coefficient on  $\text{H}_2$  (full squares, with  $[\text{He}] = 2 \times 10^{17} \text{ cm}^{-3}$ ) and He number density (open squares, with  $[\text{H}_2] = 2 \times 10^{14} \text{ cm}^{-3}$ ) measured at 300 K. The full lines are fit to the data from Figs. 3 and 4. The horizontal dotted line shows the value of the binary recombination rate coefficient  $\alpha_{\text{bin}}$  of  $\text{H}_3^+$  ions at 300 K. The dashed line shows the sum  $(\alpha_{\text{bin}} + \alpha_F)$ , i.e., maximum rate coefficient given by the sum of contributions from binary and saturated ternary recombination. The dot-dashed lines (A, B, and C) denote the sum of  $\alpha_{\text{bin}}$  and the contribution of the  $\text{H}_2$ -assisted process only (A), the sum of  $\alpha_{\text{bin}}$  and the contribution of the He-assisted process only (B), and the  $\alpha_{\text{eff}}$  arising from ternary helium-assisted recombination as predicted by the theory of Bates and Khare [24] with the ternary recombination rate coefficient of  $1.2 \times 10^{-27} \text{ cm}^6 \text{ s}^{-1}$  (C). The dotted lines denoted  $A_T$  and  $B_T$  indicate the contributions to the measured  $\alpha_{\text{eff}}$  arising from the  $\text{H}_2$ - and He-assisted ternary process, respectively. Values from other afterglow experiments are plotted using the same notation as in Fig. 4.



with the dependence predicted by classical Bates-Khare theory [24]. Values from other experiments are plotted using the same notation as in Fig. 4. Note the orders-of-magnitude difference between both ternary processes.

It is difficult to explain the third-body effects by accurate theoretical models. In this paper, we rationalize our observations by a highly simplified model that postulates the existence of long-lived H<sub>3</sub><sup>#</sup> complexes, without specifying their detailed nature and the interactions that cause these complexes to eventually decay. The basic ideas are similar to those that we have described in our previous paper [30], in which we also discuss possible other three-body mechanisms.

The lifetimes of the intermediate complexes must be very large: An estimate of the three-body coefficient  $K_{H_2}$  due to H<sub>2</sub> is given by the product of the formation rate coefficient  $\alpha_F$ , the complex lifetime  $\tau_a$ , and the rate coefficient of stabilizing collisions  $k_{S_{H_2}}$ . If one takes the formation rate coefficient as  $\alpha_F = 1.5 \times 10^{-7} \text{ cm}^3 \text{ s}^{-1}$ , and the stabilization coefficient as  $k_{S_{H_2}} = 10^{-9} \text{ cm}^3 \text{ s}^{-1}$  (a typical ion-neutral collision rate coefficient), then one needs a lifetime of  $\tau_a \sim 6 \times 10^{-7} \text{ s}$  to reproduce the experimental value  $K_{H_2} = (8.7 \pm 1.5) \times 10^{-23} \text{ cm}^6 \text{ s}^{-1}$  which can be obtained as  $K_{H_2} = \alpha_F k_{S_{H_2}} \tau_a$ . That lifetime exceeds the longest calculated [23] lifetimes of some rotational resonances ( $\sim 10^{-10} \text{ s}$ ) by a wide margin. On the other hand, some experimental studies showed that Rydberg states of the H<sub>3</sub> molecule can have lifetimes exceeding  $10^{-6} \text{ s}$  [44]. Previous treatments of this problem suggest that  $l$  mixing of the Rydberg electrons' angular momentum by either plasma electrons [33] or neutral particles [23,30,31] occurs and that it could enhance the complex lifetimes;  $l$  mixing of high Rydberg states with  $n \gtrsim 40$  due to ambient plasma electrons is indeed an exceedingly fast process: At electron densities near  $10^{11} \text{ cm}^{-3}$  mixing would occur in a time on the order of  $10^{-11}$  to  $10^{-10} \text{ s}$  for an  $n = 40$  Rydberg atom [45] and increase the lifetimes by a factor of about  $n^2$ .

The experimental data show that H<sub>2</sub> is a much more efficient third body than helium. This suggests that complex stabilization involves reactions with the ion core, which may be rotationally and perhaps vibrationally excited, rather than with the Rydberg electron. Rydberg reactions are similar to ion-molecule reactions [46,47]. Reactions with H<sub>2</sub> but not He can occur by proton or H-atom exchange that reduces the energy of the complex and eventually leads to dissociation. Uy *et al.* [48] invoke this type of reaction as the principal rotational quenching mechanism in plasmas containing He and H<sub>2</sub>.

The principal difference between He-assisted and H<sub>2</sub>-assisted recombination can be in the interaction of the Rydberg H<sub>3</sub><sup>#</sup> molecule with atomic He and with molecular H<sub>2</sub>. Particularly if we have in mind the possibility of a reactive collision of H<sub>3</sub><sup>#</sup> and H<sub>2</sub> followed by formation of H<sub>3</sub><sup>\*</sup> and its dissociation as it is described by Fermi's independent-collider model. See, e.g., recent studies of reactions of Rydberg atoms with molecules [46,47].

## V. SUMMARY AND CONCLUSIONS

The cavity ring down absorption spectrometer was used to monitor *in situ* the evolution of number densities of ortho- and para-H<sub>3</sub><sup>+</sup> during the afterglow in a He-Ar-H<sub>2</sub> gas mixture at 300 K. From these measurements the effective recombination

rate coefficient and its dependence on [He] and [H<sub>2</sub>] were determined.

A very fast H<sub>2</sub>-assisted ternary recombination was observed with the value of ternary recombination rate coefficient  $K_{H_2} = (8.7 \pm 1.5) \times 10^{-23} \text{ cm}^6 \text{ s}^{-1}$  substantially exceeding those values measured for the same ion in ambient helium ( $K_{He} \sim 10^{-25} \text{ cm}^6 \text{ s}^{-1}$ ) or predicted by the classical theory of Bates and Khare (with rate coefficient  $\sim 10^{-27} \text{ cm}^6 \text{ s}^{-1}$ ) [24]. The disagreement with the Bates and Khare theory for neutral stabilized recombination of atomic ions is not surprising. In their model, the energy of Rydberg states is only reduced by Rydberg electron-atom collisions but stabilization by collision-induced predissociation, of course, is absent. The large effect of H<sub>2</sub> most likely explains one of the remaining discrepancies in H<sub>3</sub><sup>+</sup> recombination studies, namely, the large recombination rate coefficients measured by Amano [34].

These results are not at all the typical finding in recombination studies. As far as we know, most other molecular ions recombine largely by the binary process and the environment has little effect. The sensitivity of the H<sub>3</sub><sup>+</sup> recombination to third-body effects seems to account for many of the discrepancies between experimental studies that have been conducted and clearly demonstrates the need of further theoretical work on recombination of this simplest polyatomic ion with electrons with emphasis on formation of long-lived collisional complexes and on the influence of third particles on the overall recombination. An existence of a similar ternary process for D<sub>3</sub><sup>+</sup> ions with D<sub>2</sub> as the third particle is expected. We are not able to predict to what extent the H<sub>2</sub>-assisted ternary process may have influenced recombination rates of other ions measured in plasma afterglows. The required lifetimes of the metastable Rydberg states formed in the proposed recombination process are quite long; therefore the ions recombining via direct mechanism [49] should not be affected. However, the recombination rate coefficients of some ions recombining via the indirect recombination mechanism obtained in the afterglow experiments could have been enhanced by fast ternary He- or H<sub>2</sub>-assisted recombination. Possibly affected ions are HCO<sup>+</sup> and N<sub>2</sub>H<sup>+</sup>, as both of them recombine by the indirect mechanism [50] and the reported results of the afterglow experiments differ by almost an order of magnitude (see Fig. 2 in [51]). Moreover, the highest recombination rate coefficients for both of these ions were reported by Amano, who measured in H<sub>2</sub> buffer gas [34].

A fast H<sub>2</sub>-assisted ternary recombination may directly impact models describing hydrogen plasmas and it can have consequences in plasma physics including physics of discharges, astrophysics, recombination pumped lasers, plasma spectroscopy, plasmatic technologies, etc. It can also influence processes in ionospheres of large planets with relatively high pressure of H<sub>2</sub>, e.g., Jupiter and Jupiter-like planets, and may be important for chemistry of gas giant exoplanets.

Further measurements at different temperatures are in progress.

## ACKNOWLEDGMENTS

This work was partly supported by Czech Science Foundation projects GACR P209/12/0233 and GACR 14-14649P, and by Charles University in Prague projects GAUK 659112, GAUK 692214, UNCE 204020/2012 and SVV 260 090.

- [1] K. N. Crabtree *et al.*, *Astrophys. J.* **729**, 15 (2011).
- [2] M. Larsson and A. Orel, *Dissociative Recombination of Molecular Ions* (Cambridge University, Cambridge, 2008).
- [3] R. Johnsen and S. L. Guberman, in *Advances In Atomic, Molecular, and Optical Physics*, edited by E. Arimondo, P. Berman, and C. Lin, Vol. 59 (Academic, New York, 2010), pp. 75–128.
- [4] D. R. Bates, M. F. Guest, and R. A. Kendall, *Planet. Space Sci.* **41**, 9 (1993).
- [5] W. D. Watson, *Astrophys. J.* **183**, L17 (1973).
- [6] E. Herbst and W. Klempner, *Astrophys. J.* **185**, 505 (1973).
- [7] S. C. O. Glover and D. W. Savin, *Mon. Not. R. Astron. Soc.* **393**, 911 (2009).
- [8] T. Oka, *Phys. Rev. Lett.* **45**, 531 (1980).
- [9] P. Drossart *et al.*, *Nature (London)* **340**, 539 (1989).
- [10] S. Miller, T. Stallard, J. Tennyson, and H. Melin, *J. Phys. Chem. A* **117**, 9770 (2013).
- [11] T. R. Geballe and T. Oka, *Nature (London)* **384**, 334 (1996).
- [12] T. Oka, *Proc. Natl. Acad. Sci. USA* **103**, 12235 (2006).
- [13] V. Kokoouline, C. H. Greene, and B. D. Esry, *Nature (London)* **412**, 891 (2001).
- [14] V. Kokoouline and C. H. Greene, *Phys. Rev. A* **68**, 012703 (2003).
- [15] S. Fonseca dos Santos, V. Kokoouline, and C. H. Greene, *J. Chem. Phys.* **127**, 124309 (2007).
- [16] B. J. McCall *et al.*, *Nature (London)* **422**, 500 (2003).
- [17] H. Kreckel *et al.*, *Phys. Rev. Lett.* **95**, 263201 (2005).
- [18] B. J. McCall *et al.*, *Phys. Rev. A* **70**, 052716 (2004).
- [19] A. Wolf *et al.*, *Phil. Trans. R. Soc. A* **364**, 2981 (2006).
- [20] A. Petignani *et al.*, *Phys. Rev. A* **83**, 032711 (2011).
- [21] P. Rubovic *et al.*, *J. Phys. Chem. A* **117**, 9626 (2013).
- [22] J. Glosik *et al.*, *J. Phys. B* **41**, 191001 (2008).
- [23] J. Glosík, R. Plašil, I. Korolov, T. Kotřík, O. Novotný, P. Hlavenka, P. Dohnal, J. Varju, V. Kokoouline, and C. H. Greene, *Phys. Rev. A* **79**, 052707 (2009).
- [24] D. Bates and S. Khare, *Proc. Phys. Soc. Lond.* **85**, 231 (1965).
- [25] R. J. Saykally, E. A. Michael, J. Wang, and C. H. Greene, *J. Chem. Phys.* **133**, 234302 (2010).
- [26] R. Plasil *et al.*, *Int. J. Mass Spectrom.* **218**, 105 (2002).
- [27] P. Macko *et al.*, *Int. J. Mass Spectrom.* **233**, 299 (2004).
- [28] J. Varju, M. Hejduk, P. Dohnal, M. Jilek, T. Kotřík, R. Plasil, D. Gerlich, and J. Glosik, *Phys. Rev. Lett.* **106**, 203201 (2011).
- [29] O. Novotny *et al.*, *J. Phys. B* **39**, 2561 (2006).
- [30] R. Johnsen *et al.*, *J. Phys. Chem. A* **117**, 9477 (2013).
- [31] J. Glosik *et al.*, *Molec. Phys.* **108**, 2253 (2010).
- [32] P. Dohnal *et al.*, *J. Chem. Phys.* **136**, 244304 (2012).
- [33] T. Gougousi, R. Johnsen, and M. F. Golde, *Int. J. Mass Spectrom.* **149–150**, 131 (1995).
- [34] T. Amano, *J. Chem. Phys.* **92**, 6492 (1990).
- [35] P. Hlavenka *et al.*, *Int. J. Mass Spectrom.* **255**, 170 (2006).
- [36] C. M. Lindsay and B. J. McCall, *J. Mol. Spectrosc.* **210**, 60 (2001).
- [37] L. S. Rothman *et al.*, *J. Quant. Spectrosc. Radiat. Transfer* **110**, 533 (2009).
- [38] J. Glosik *et al.*, *Plasma Sci. Technol.* **12**, S117 (2003).
- [39] J. A. MacDonald, M. A. Biondi, and R. Johnsen, *Planet. Space Sci.* **32**, 651 (1984).
- [40] K. Hiraoka, *J. Chem. Phys.* **87**, 4048 (1987).
- [41] M. T. Leu, M. A. Biondi, and R. Johnsen, *Phys. Rev. A* **8**, 413 (1973).
- [42] D. Smith and P. Spanel, *Int. J. Mass Spectrom.* **129**, 163 (1993).
- [43] S. Laube *et al.*, *J. Phys. B* **31**, 2111 (1998).
- [44] C. Bordas and H. Helm, *Phys. Rev. A* **47**, 1209 (1993).
- [45] S. K. Dutta, D. Feldbaum, A. Walz-Flannigan, J. R. Guest, and G. Raithel, *Phys. Rev. Lett.* **86**, 3993 (2001).
- [46] S. Yu *et al.*, *J. Chem. Phys.* **140**, 034310 (2014).
- [47] H. Song *et al.*, *J. Chem. Phys.* **123**, 074314 (2005).
- [48] D. Uy, C. M. Gabrys, M.-F. Jagod, and T. Oka, *J. Chem. Phys.* **100**, 6267 (1994).
- [49] D. R. Bates, *Phys. Rev.* **78**, 492 (1950).
- [50] S. Fonseca dos Santos, N. Douguet, V. Kokoouline, and A. E. Orel, *J. Chem. Phys.* **140**, 164308 (2014).
- [51] V. Poterya, J. L. McLain, N. G. Adams, and L. M. Babcock, *J. Phys. Chem. A* **109**, 7181 (2005).